The Infrared and Ultraviolet Spectra of Individual Conformational Isomers of Biomolecules: Tryptamine

Joel R. Carney and Timothy S. Zwier*

Department of Chemistry, Purdue University, West Lafayette, Indiana 47907-1393

Received: April 14, 2000; In Final Form: July 10, 2000

Resonant ion-dip infrared (RIDIR) and UV−UV hole-burning spectroscopies are used to record the hydride stretch infrared spectra and $S_1 \leftarrow S_0$ ultraviolet spectra of each of seven conformational isomers of tryptamine free from interference from one another. The different conformations of the ethylamine side chain produce unique $S_1 \leftarrow S_0$ vibronic spectra, which can serve as the basis for RIDIR spectroscopy. The seven conformers possess unique spectral signatures in the alkyl CH stretch region of the infrared, which aid in the assignment of the observed transitions in the ultraviolet. Density functional theory (DFT) calculations of the structures, relative energies, and harmonic vibrational frequencies of nine low-energy minima are compared with the present and previous experimental data on tryptamine to assign the spectra of all seven conformers, all of which point the α carbon out of the plane of the indole ring. The nine conformers consist of all combinations of the three minimum-energy amino group *positions* (anti, gauche toward the phenyl side, and gauche toward the pyrrole side of indole) and three amino group *orientations* (180°, ±60°) at each position. All three anti conformers are observed experimentally, whereas only the two lowest-energy of the three orientational conformers at each gauche position are observed. The dominant factor in determining the form of the CH stretch infrared spectrum is the orientation of the amino group, with the amino group position playing a secondary role. The frequencies of the $S_1 \leftarrow S_0$ origin transitions, on the other hand, are most sensitive to the position of the amino group, whether it is anti, gauche phenyl, or gauche pyrrole. The prospects for using these methods more generally to characterize the conformations and energetics of flexible biomolecules are discussed.

Introduction

One of the foundations of molecular biology is the notion that most proteins adopt a single, preferred structure that is optimized for their chemical or physical function. This preference for a single structure occurs despite the staggering number of local minima that are energetically accessible to the protein. A delicate balance of intraprotein, protein−solvent, and solvent−solvent effects directs the conformational preferences of these large biopolymers. The vestiges of this complex conformational landscape can be seen even in small molecules containing only a few points of flexibility. When such small molecules are among nature's building blocks, it is crucial to quantitatively account for and understand their conformational preferences as a foundation to the study of larger macromolecules. The recent improvements in molecular mechanics force fields by MacKerell et al.[1,2] and Friesner and co-workers[3−11] are two examples of the tremendous progress that is accompanying such efforts. Crucial to their quantitative success are benchmark experimental data and ab initio calculations against which the empirical force fields can be rigorously tested. Much of the experimental data used to test empirical force fields has been solution-phase data, as expected. However, the types of tests that these studies can provide are restricted in cases where many conformers exist in solution. The substantial thermal energy of the conformers produces congested and highly overlapped optical spectra, and their rapid interconversions can confound their detection via NMR spectroscopy.

The interpretation of solution-phase data requires a careful analysis of solvent effects. To separate the intramolecular and solvent contributions to the conformational preferences, it would be helpful to build up an analogous body of data on the conformational preferences and populations of the isolated molecules themselves. The present study contributes to the growing body of such data,[12−30] combining conformation-specific infrared and ultraviolet spectroscopy with density functional theory (DFT) calculations on tryptamine (TRA), a close analogue of both tryptophan and serotonin that contains a flexible ethylamine side chain.

Over the past decade or more, supersonic expansion cooling has been used as a means to resolve the spectral consequences of conformational complexity in the gas phase.[13−30] In the expansion, the conformations that are significantly populated at the preexpansion nozzle temperature are cooled by collisions in the expansion into the zero-point levels associated with the various conformational minima. The conformational populations are determined by (1) the relative energies of the conformational minima, (2) the barriers between them, and (3) each conformer's collision-induced folding dynamics. When the sample molecule contains an ultraviolet chromophore, each conformation possesses its own unique electronic spectrum. $S_1 \leftarrow S_0$ origin transitions shift slightly in frequency depending on the structure of each conformation, and transition intensities reflect the relative populations of the conformers in the downstream expansion.

The ground-state vibrational spectroscopy of individual conformers has received much less attention. Infrared spectra

* To whom correspondence should be addressed.

10.1021/jp001433r CCC: $19.00
Published on Web 09/01/2000

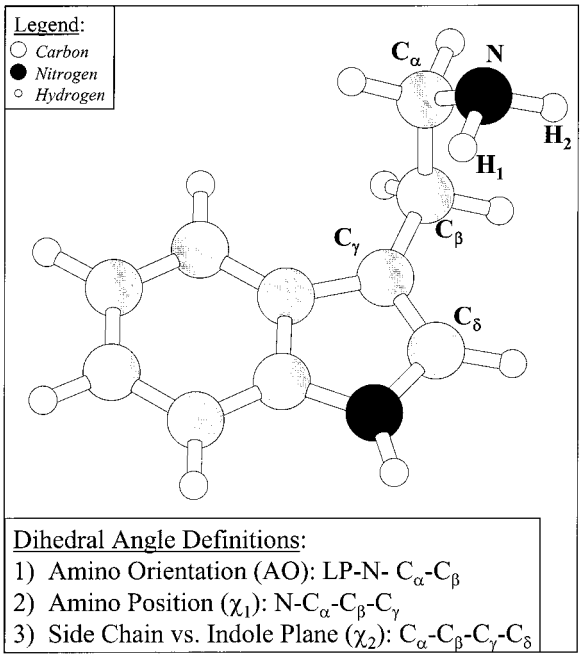

Figure 1. A picture of the tryptamine molecule. Atom labels and dihedral angles are presented to guide the reader.

are often plagued by overlapping IR transitions and the lack of a ready means of selecting a single conformation. Felker and co-workers have made strides in this field by using ionization-loss stimulated Raman spectroscopy (ILSRS), a double-resonance method in which the Raman transitions are detected indirectly by the depletions they produce in the resonant two-photon ionization signal of an individual conformer.[31,32] The present work shows the usefulness of the infrared analogue of this method,[33] referred to here as resonant ion-dip infrared spectroscopy (RIDIRS). RIDIRS has served as a powerful probe of the structures of aromatic-(water)$_n$ clusters via the hydride stretch region of the infrared, where the OH and NH stretch fundamentals are sensitive to the number, type, and strengths of hydrogen bonds in which they are involved.[34−40] In RIDIRS, the inherent mass and wavelength selectivity of the resonant two-photon ionization (R2PI) step enables one to monitor the ion signal selectively from a single conformation. The infrared spectrum of each conformer can then be studied by monitoring the IR-induced depletions in this signal as a function of IR wavenumber in the hydride stretch region (2800−3800 cm^{-1}).

Tryptamine serves as a valuable testing ground for conformation-specific infrared spectroscopy. Its structure is shown in Figure 1, along with the atom labeling and angle definitions used in the present work. TRA has served as a simpler analogue of tryptophan in which conformational flexibility and its relevance to indole photophysics can be tested.[23,27,29] TRA has importance in its own right as a neurotransmitter that is effective in curing migraine headaches.[41] Furthermore, TRA bears a close structural and chemical similarity to the neurotransmitter serotonin (5-hydroxytryptamine) and to melatonin (5-methoxy-*N*-acetyltryptamine), which plays a key role in the daily behavioral and physiological states of humans. In all three molecules, the conformational flexibility of the ethylamine or *N*-acetyl-ethylamine side chain plays an important role in its binding to receptor sites.

More than a decade ago, the Levy group carried out an extensive set of studies of the ultraviolet spectroscopy of jet-cooled tryptamine and other tryptophan derivatives.[23,27,29] A total of seven conformer origins were identified in the $S_1 \leftarrow S_0$ spectrum of tryptamine, five of which were well-resolved. The other two origins appeared as a single, overlapped band in the low-resolution spectrum.[29] Ensuing high-resolution studies found the two origins to be split by only 0.611 cm^{-1}.[27] All of these bands were studied with partial rotational resolution, and all but the overlapped bands were fit to obtain rotational constants for the conformers in both the ground and the excited states. By constraining the lengths and orientations of the bonds in the ethylamine side chain, Philips et al.[27] made assignments of several of the observed bands. Oddly enough, two of the bands were fit to structures in which the amino group was eclipsed with the hydrogens on the β carbon. Subsequently, these authors used deuterium substitution on the amino group to make a tentative assignment of the amino group orientation for some of the conformers.[23] The rotational coherence studies of Felker and co-workers have since added to and refined these deductions.[22]

In the present work, we employ RIDIR and UV−UV hole-burning spectroscopies to build on previous results in making a complete conformational assignment of the UV spectrum of tryptamine. It appears now that the seven observed conformers belong to a family of nine conformational minima which share an out-of-plane orientation for the side chain but differ in the 3-fold positions and 3-fold orientations of the amino group. Tryptamine thus provides a venue for testing the sensitivity of the alkyl CH stretch vibrations to these conformational changes. It is not obvious that the CH stretch vibrations would be sensitive to such conformational changes. However, we were encouraged to pursue this possibility by recent results on methanol-containing clusters, which showed that the methyl CH stretches shift characteristically with the nature of the H-bonding occurring at their OH group (whether donor, acceptor, or donor−acceptor).[42]

The RIDIR spectra presented here demonstrate the potential of the CH stretch infrared spectrum for distinguishing individual conformations of small biomolecules with conformational flexibility. We will see that the CH stretch infrared spectra are complementary to rotational spectroscopy in that they are most sensitive to the *orientation*, rather than the *position*, of the amino group.

II. Methods

A. Experimental. Our experimental apparatus and methods have been described in detail elsewhere.[43] The tryptamine sample (98% pure, Aldrich) was entrained in the expansion by heating the sample in a modified version of our solenoid-based pulsed valve (0.8-mm-diam pinhole, 20 Hz) capable of heating to above 200 °C. As shown in Figure 2, the sample compartment was contained in a brass block extension to the pulsed valve. Poppits of extended length (PEEK) are used to make the seal on the front face of the block. A cartridge heater is used to heat the sample (140 °C) and orifice area without directly heating the solenoid area of the pulsed valve. This extension enables us to run the pulsed valve without sample buildup around the operating components, which can degrade valve performance. Samples are also interchanged or refilled easily. Most importantly, the sample can be heated above the operating temperature of the solenoid and the normal, temperature-induced instability in the pulsed valve operation is diminished.

The tryptamine sample is entrained in a 70% neon, 30% helium mixture at 1.5 bar total pressure. Tryptamine vapor pressure constitutes about 0.01% of the gas mixture. The expansion is skimmed before the clusters enter the ion source region of a linear time-of-flight mass spectrometer.

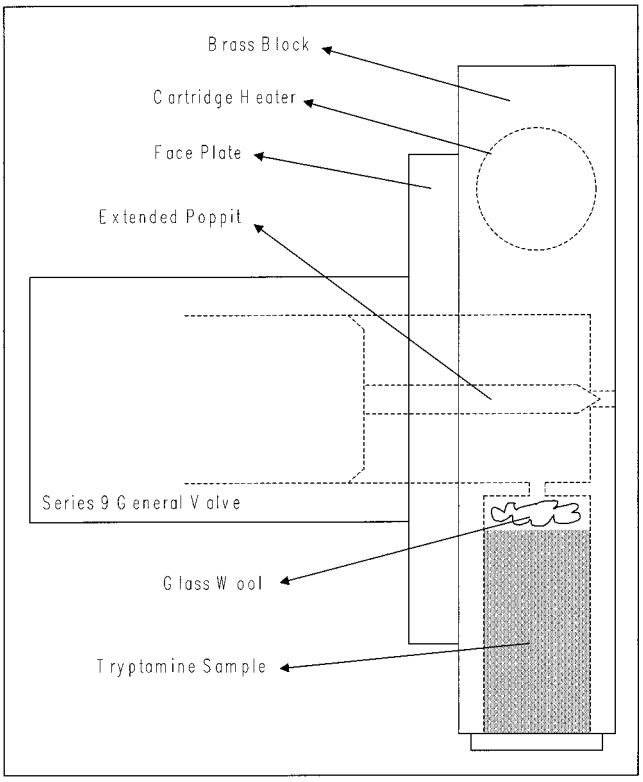

Figure 2. A picture of the sample cell used in this work. A brass block is attached to the faceplate of a standard pulsed general valve. The TRA sample is inserted into this block and heated by a cartridge heater. A custom, extended poppit seals at the 0.8 mm exit pinhole of the brass block.

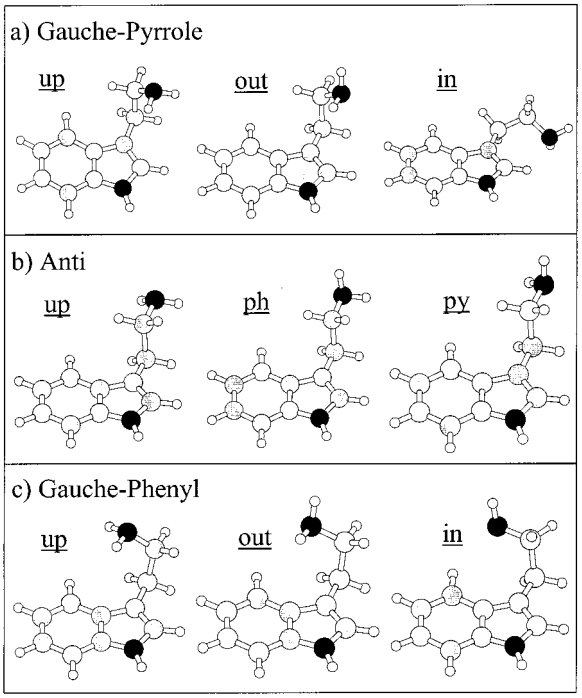

Figure 3. Pictorial summary of the calculated structural minima for TRA. The nine species are separated into three groups, which differ by the amino position of the ethylamine side chain relative to indole: (a) gauche near the pyrrole side of indole, (b) anti, and (c) gauche near the phenyl side of indole. The designations within each subgroup describe the position of the amino lone pair relative to the indole ring, or the amino orientation. The χ_1 values for "out", "in", "py", and "ph" are nominally $\pm 60°$, while "up" distinguishes the structures for which the amino orientation is 180°.

This work employs a combination of methods, which have as their starting point mass-selected, one-color R2PI spectroscopy. The doubled output of an Nd:YAG-pumped dye laser operating at 20 Hz is used as the ionization source, with mass selection via linear time-of-flight methods. Typical unfocused UV output is 0.5 mJ/pulse (using Rhodamine 590).

To record the size and conformer-specific infrared spectrum of a single conformer, the mass and wavelength selectivity offered by R2PI is used as part of a double-resonance technique, which we refer to as resonant ion-dip infrared spectroscopy (RIDIRS). The infrared output of a seeded Nd:YAG-pumped, KTA-based optical parametric converter operated at 10 Hz is spatially overlapped with the R2PI laser, preceding the UV by 200 ns. The UV source, operating at 20 Hz, is fixed to a desired vibronic transition, creating a constant ion signal. The IR source is scanned through the desired IR region of interest. When an infrared transition of the selected conformer is encountered, its ground state population, and thus the constant ion signal, is depleted. The difference between the ion signal with and without the IR present is monitored via active baseline subtraction methods and interfaced with a personal computer.

The R2PI spectra of the different conformers appear in the same mass channel, leading to intermingled spectra that must be separated from one another. UV−UV hole-burning can be used to identify all the UV vibronic transitions due to a single species in the R2PI spectrum. To achieve such selection, one UV laser is used as a hole-burning source, fixed on a particular transition. The hole-burning spectrum is then recorded by tuning a time-delayed, probe UV source through the R2PI spectrum while monitoring the difference in ion intensity with and without the hole-burning laser present. All vibronic transitions that arise from the ground-state responsible for the unique UV transition will show up as depletions in the hole-burning spectrum. Both RIDIR and hole-burning spectra are plotted as positive-going signals in this work.

B. Computational. Density functional theory calculations of the tryptamine structures, energies, harmonic vibrational frequencies, rotational constants, and infrared intensities were carried out in Gaussian 98[44] using the Becke3LYP functional.[45,46] Geometry optimizations of the TRA conformer structures were performed, using both a 6-31+G*(5d)[47] basis set and the aug-cc-pVDZ[48] correlation-consistent basis set of Dunning. The large Dunning basis set provided a check on the reliability of the lower level calculations in determining structures and relative energies of the conformers. Using the 6-31+G*(5d) basis set we computed harmonic vibrational frequencies and infrared intensities for each of the nine lowest-energy conformational minima. The locations of true minima were confirmed by the lack of imaginary frequencies in the vibrational frequency calculations.

III. Results and Analysis

A. Calculated Structures and Relative Energies of the Conformers. Figure 3 presents the structures of the nine conformational isomers whose minima were located via the present calculations. Guided by previous experiments on tryptamine and phenethylamine,[13,14,22,23,49] we explored only conformers that possessed an out-of-plane $C_\alpha H_2-NH_2$ tail. The nine conformational minima then differ in the position of the amino group (anti, Figure 3b; gauche on the pyrrole side, Figure 3a; and gauche on the phenyl side, Figure 3c) and its orientation (lone pair up, out away from, and in toward the indole cloud). Notably, no minima in which the amino group was eclipsed

TABLE 1: Summary of Selected Structural Parameters of the Nine Lowest Energy Minima Calculated for Tryptamine at the DFT Becke3LYP/6-31+G*(5d) and /aug-cc-pVDZ Levels of Theory[a]

							rotational constants (GHz)		
Description[b]	$C_\gamma-C_\beta$	$C_\beta-C_\alpha$	$C_\alpha-N$	NH_2 orientation[c] ψ	χ_1[d]	χ_2[e]	A''	B''	C''
	angstroms			degrees					
Gpy(out)	1.504/1.503	1.541/1.538	1.468/1.468	56.1/57.4	63.8/64.6	76.6/77.1	1.740/1.745	0.663/0.662	0.538/0.537
Gpy(up)	1.502/1.501	1.551/1.548	1.463/1.463	−178.5/−177.8	62.7/63.4	75.3/76.5	1.718/1729	0.662/0.660	0.537/0.535
Anti(py)	1.503/1.502	1.539/1.537	1.470/1.470	−54.0/−54.7	179.3/179.8	76.0/75.8	1.785/1.781	0.601/0.602	0.468/0.469
Anti(up)	1.503/1.502	1.549/1.546	1.465/1.465	180.8/181.0	−178.6/−178.7	77.4/77.4	1.775/1.774	0.601/0.601	0.468/0.468
Anti(ph)	1.503/1.502	1.539/1.537	1.469/1.469	54.1/54.9	−176.3/−176.5	76.4/76.5	1.777/1.778	0.604/0.604	0.469/0.469
Gph(out)	1.506/1.505	1.541/1.538	1.468/1.468	−54.5/−56.0	−65.6/−65.9	85.3/85.6	1.582/1.584	0.742/0.741	0.550/0.550
Gph(up)	1.505/1.504	1.551/1.548	1.463/1.463	177.9/177.6	−61.6/−61.9	93.5/93.0	1.605/1.605	0.716/0.716	0.548/0.548
Gph(in)	1.506	1.545	1.471	46.9	−82.9	66.2	1.534	0.747	0.523
Gpy(in)	1.507	1.535	1.473	−58.6	66.6	149.8	2.332	0.565	0.463

[a] Values are presented for both levels of theory where applicable: low/high (6-31+G*/aug-cc-pVDZ). The $C_\alpha-C_\beta-C_\gamma$ angle for each of the structures was 114°(±0.5°). [b] The amino position of each conformer is stated in the first portion of the description (Gpy = gauche, toward pyrrole; Gph = gauche, toward phenyl; or Anti), and the amino orientation is denoted in parentheses by the direction of the amino lone pair in reference to the indole chromophore (see Figure 3 for pictorial representation of the structures). [c] The amino orientation (ψ) is described by a dihedral angle involving the amino lone pair, the amino nitrogen, C_α, and C_β. The position of the lone pair was deduced by bisecting the $H-N-C_\alpha-C_\beta$ angles of the two hydrogen atoms and rotating 180°. The amino group orientation angle for the structure in Figure 1 is nominally 180° (or "up"). A positive rotation of the amino group, looking from N to C_α down the $N-C_\alpha$ bond, would be in the counterclockwise direction. [d] The amino position is represented by the second dihedral ($N-C_\alpha-C_\beta-C_\gamma$), χ_1. Positive rotation of the amino position is counterclockwise, looking from C_α to C_β, and 180° corresponds to the amino group in the anti position. [e] The third dihedral (χ_2) describes the degree to which the side chain is planar with indole ($C_\alpha-C_\beta-C_\gamma-C_\delta$). A value of 0° is assigned when C_α is in the indole plane toward the pyrrole moiety of indole. A positive rotation, looking from C_γ to C_β down the C_γ-C_β bond, is defined by a counterclockwise rotation.

with the β carbon hydrogens were found at either level of theory.

Table 1 summarizes the key structural parameters of these nine TRA conformers for both basis sets used, the 6-31+G*-(5d) and the aug-cc-pVDZ. Bond lengths are presented for the heavy atom distances in the ethylamine side chain. Dihedral angles that describe the structure of the ethylamine side chain are also provided and are based on the definitions in Figure 1, following a convention similar to that used by Sipior and Sulkes.[18] The structures used in this work differ from those of Levy and co-workers by rotation of 180° about the $C_\beta-C_\gamma$ bond.[27]

To specify the amino group position, structures will be referred to using a shorthand notation, as 'Gpy' (for gauche, pyrrole side), 'anti', or 'Gph' (gauche, phenyl side). Within each position, the amino group orientation, whether 'up', 'in' (toward the indole cloud), or 'out' (away from the indole π cloud), is added to the designation for the gauche species. For the anti conformers, an 'up', 'py', or 'ph' designation is used to distinguish the lone pair pointing up, toward the pyrrole side, or toward the phenyl side of indole, respectively (Figure 3).

The entries in Table 1 are divided into sets of conformational structures that differ primarily in the amino group *position*, and thus share similar rotational constants. Two of the nine structures, the Gpy(in) and the Gph(in), are pulled aside as a separate subgroup because they both suffer from a destabilizing interaction of the lone pair on the amino group with the indole π cloud. This interaction significantly distorts the ethylamine side chain relative to the other seven structures.

Table 2 summarizes the relative energies (kcal/mol) of the calculated conformers, both with and without ZPE correction. The use of the aug-cc-pVDZ basis set changes the relative energies of the conformers by no more than 0.18 kcal/mol from their uncorrected values using the 6-31+G*(5d) basis set. This fact supports the adequacy of the smaller basis set in calculations of this kind. ZPE corrections change the relative energies by similar amounts (<0.2 kcal/mol). Given the close energies of several of the conformers, the ZPE correction leads to a reordering of the energies of some of these structures. However, the exact energy ordering of close-lying structures is unimportant for much of what follows. ZPE corrections to the conformer

TABLE 2: Relative Energies of the Nine Structural Minima of TRA Calculated at the DFT Becke3LYP/6-31+G* and aug-cc-pVDZ Levels of Theory

	relative energy (kcal/mol)			
	6-31+G*		aug-cc-pVDZ	
description		ZPE corr		ZPE corr[b]
Gpy(out)	0.000	0.000	0.000	0.000
Gpy(up)	0.267	0.186	0.315	0.234
Anti(py)	0.759	0.620	0.573	0.435
Anti(up)	0.611	0.448	0.581	0.419
Anti(ph)	0.760	0.562	0.584	0.386
Gph(out)	0.553	0.553	0.572	0.572
Gph(up)	0.832	0.798	0.947	0.913
Gph(in)	2.683	2.502		
Gpy(in)	1.198	1.174		

[a] See Table 1 or text for conformer descriptions [b] Zero-point energy corrections from 6-31+G* frequency calculations are used.

energies found with the aug-cc-pVDZ basis set are taken from the 6-31+G*(5d) frequency calculations.

At both levels of theory, whether with or without ZPE corrections, two of the nine minima are substantially less stable than the other seven. These are the same two (nominally) gauche structures (Gpy(in) and Gph(in)) identified earlier as having the nitrogen lone pair pointed in toward the π cloud from either the pyrrole or the phenyl side (Figure 3a-in and 3c-in, respectively), destabilizing them relative to the others. In contrast, the global minimum structure is consistently the structure shown in Figure 3a-out, the corresponding gauche− pyrrole structure in which the nitrogen lone pair is oriented away from the π cloud. In this orientation, the gauche structures provide additional stabilization of the side chain, presumably through a weak hydrogen bond between the amino hydrogen and the indole π cloud. The Gpy(up) structure shown in Figure 3a-up is second in energy, only 0.315 (0.234) kcal/mol above Gpy(out).

Not surprisingly, the three anti structures (Figure 3b), which place the amino group far from indole, are close in energy to one another, with Figure 3b-py and Figure 3b-ph effectively degenerate. The remaining two gauche phenyl structures (Figure 3c-up and Figure 3c-out, labeled as Gph(up) and Gph(out),

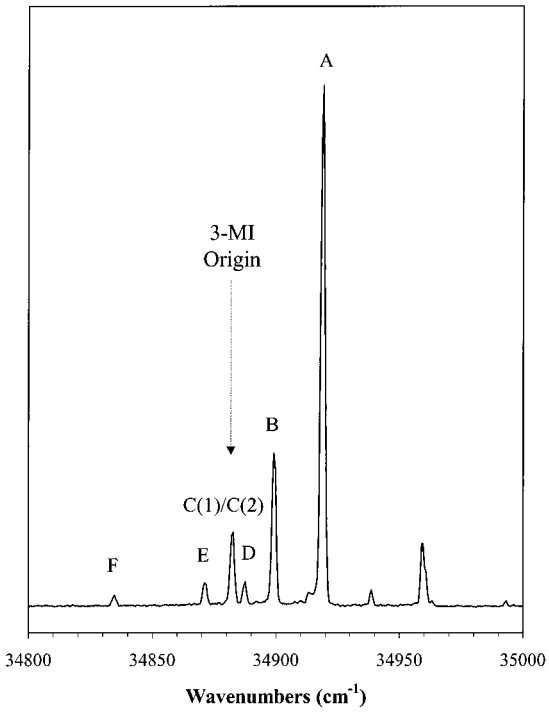

Figure 4. A one-color resonant two-photon ionization spectrum in the $S_1 \leftarrow S_0$ origin region of the TRA^+ mass channel. The same letter designations of seven origins due to different conformational isomers of TRA are included from previous studies (see text). The C(1)/C(2) label reminds us that there are two origins in this region, unresolved in the present spectrum. The position of the 3-methylindole (3-MI) $S_1 \leftarrow S_0$ origin at 34 877 cm^{-1} is included for comparison.

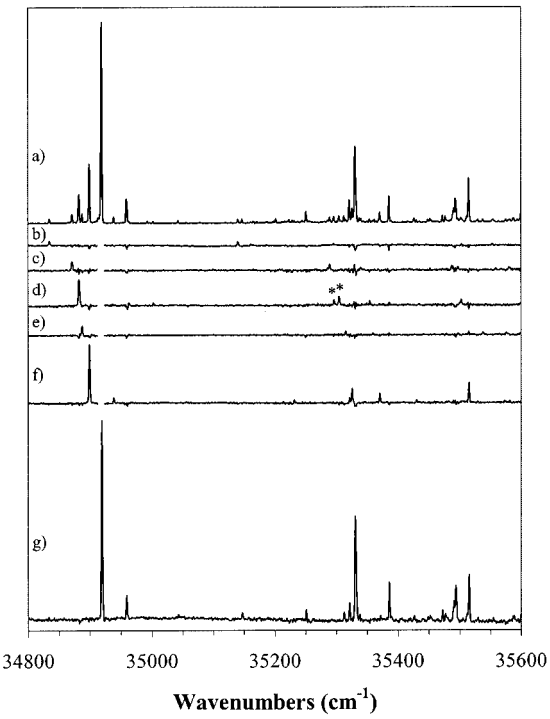

Figure 5. (a) One-color resonant two-photon ionization spectrum in the TRA^+ mass channel. (b−g) UV−UV hole-burning spectra of conformers F, E, C, D, B, and A, respectively. The region near the A origin was removed from spectra (b−f) because of the inherent noise encountered when scanning through a region with a large ion signal. Two vibronic transitions in part (d) are highlighted with an asterisk and will be used to distinguish the two "C" conformers using RIDIR spectroscopy.

respectively) are comparable in energy to the anti structures, presumably because of a less favorable π H-bonding interaction of the amino hydrogens with the phenyl side of the indole ring than with the pyrrole side.

B. R2PI and UV−UV Hole-Burning Spectra. Figure 4 presents a one-color R2PI spectrum of the $S_1 \leftarrow S_0$ origin region of tryptamine cooled in a supersonic expansion. The spectrum, in terms of both frequencies and intensities of transitions, is virtually identical to that of Park et al.[29] The letter designations used to label the transitions are also adopted from that work, in which six different origins were assigned as a result of power saturation studies (labeled A−F). The spectrum is dominated by a strong origin at 34 919 cm^{-1}, labeled "A". In addition, high-resolution studies determined that transition C is actually composed of two overlapping origins (split by 0.611 cm^{-1}) due to different conformers.[27] The C(1)/C(2) label in Figure 4 reminds us that two unresolved transitions make up C (C(1) and C(2)), leading to a total of seven distinct origins. The position of the 3-methylindole (3-MI) origin is added for comparison (34 877 cm^{-1}).

The UV−UV hole-burning spectra of Figure 5 present confirming evidence that the resolved transitions in Figure 4 are due to different ground state conformations of tryptamine. In Figure 5a, an overview R2PI spectrum extending almost 700 cm^{-1} above the A origin is presented. Figure 5b−g presents the corresponding UV−UV hole-burning spectra over the same region, with the hole-burning laser set to transitions F, E, C, D, B, and A, respectively. The R2PI spectrum neatly divides into subspectra upon hole-burning, accounting for all observed transitions in the region. Because the hole-burning spectra are recorded as the difference in ion signal with and without the hole-burning laser present, noise levels increase when large transitions are encountered. This increase is most noticeable in the region near the A origin, which has been removed in the other hole-burning spectra for clarification.

Table 3 summarizes the frequencies and relative intensities of the vibronic transitions in each of these conformation-specific UV spectra. Because the C transition is an unresolved set of two transitions, the hole-burning spectrum of this "C" peak did not separate the UV spectra of these two species. We will return to the analysis of this spectrum after making assignments of the spectra to individual conformers. Clearly, however, the frequencies and intensities of the low-frequency bands vary from one isomer to another, as one would anticipate if much of this low-frequency vibrational structure is due to large amplitude motion of the ethylamine side chain.

C. RIDIR Spectroscopy. The R2PI and hole-burning spectra of Figure 5 provide a basis for recording conformation-specific IR spectra in the hydride stretch region using RIDIR spectroscopy. In the $S_1 \leftarrow S_0$ origin region, only transition C is a blend of transitions due to different conformers. Figure 6a shows the RIDIR spectrum of band C, which is thereby the sum of two IR spectra due to the two conformers that contribute to the R2PI signal. However, the UV−UV hole-burning spectrum of band C (Figure 5d) possesses two bands identified in the region 410−430 cm^{-1} above origin C, where only a single band appeared in most of the other conformer spectra. These two bands are marked by asterisks in Figure 5d. There was sufficient ion signal to record RIDIR spectra of these two bands, which are shown in Figure 6b,c. A comparison of the RIDIR spectrum of band C (Figure 6a) with the spectra of Figure 6b,c shows that the former spectrum is indeed a composite of the latter two. Thus, the spectra of Figure 6b,c are the IR spectra of the individual conformers (hereafter labeled C(1) and C(2)), free from interference from one another.

TABLE 3: Summary of the Transition Frequencies and Relative Intensities Deduced from the UV−UV Hole-Burning Spectra

origin[a]	transition[b]	relative position[c]	relative intensity[d]
A	34 919	0	100
	34 960	41	12.1
	35 148	229	2.2
	35 251	332	5.8
	35 313	394	3.6
	35 322	403	11.4
	35 331	412	37.9
	35 386	467	13.3
	35 472	553	3.5
	35 494	575	12
	35 515	596	22.1
B	34 899	0	29.4
	34 939	40	3.2
	35 232	333	0.9
	35 326	427	7.2
	35 371	472	5.3
	35 430	531	1.4
	35 618	719	8.7
C	34 883	0	14.3
	35 003	120	0.8
	35 296	413	3.1
	35 305	422	3.2
	35 354	471	1.8
	35 503	620	2.5
	35 602	719	3.6
D	34 888	0	4.8
	35 315	427	1.9
	35 538	650	1.7
	35 575	687	1.7
E	34 872	0	4.3
	35 290	418	2.8
	35 341	469	1.8
	35 497	625	1
	35 580	708	1
F	34 835	0	2.2
	35 140	305	1.9
	35 296	461	1
	35 503	668	0.5
	35 553	718	1

[a] $S_1 \leftarrow S_0$ origin transition selected in hole-burning scan (see Figure 5). [b] Vibronic transition selected from hole-burning scans (in cm^{-1}). [c] Relative position of the vibronic transition from its respective origin (in cm^{-1}). [d] Intensities determined by peak heights; intensity of 'A' arbitrarily set to 100.

To facilitate direct comparison, Figure 7 (conformers A, C(2), C(1), and D) and Figure 8 (conformers B, E, and F) bring together the RIDIR spectra of the seven observed conformers of tryptamine. These conformation-specific infrared spectra are the most important results of the present study.

All seven spectra are dominated by the N−H stretch fundamental of the indole moiety, which appears at 3524 ± 1 cm^{-1}, unchanged from one isomer to the next. This is not surprising given the fact that the ethylamine side chain is not long enough to reach near the indole N−H group in any of the conformers of Figure 3.

The N−H stretch fundamentals associated with the amino group on the ethylamine side chain are difficult to observe because of their weak intensity in the infrared. Only in isomer A, where the larger ion signal enabled more sensitive searches for these transitions, was positive identification made. The inset of Figure 7a shows the pair of transitions observed when the IR power was significantly increased, taken with about 25 times greater sensitivity. Based on the calculated frequencies of the amino NH stretch modes, the transition at 3405 cm^{-1} is assigned as the antisymmetric stretch fundamental, while the symmetric

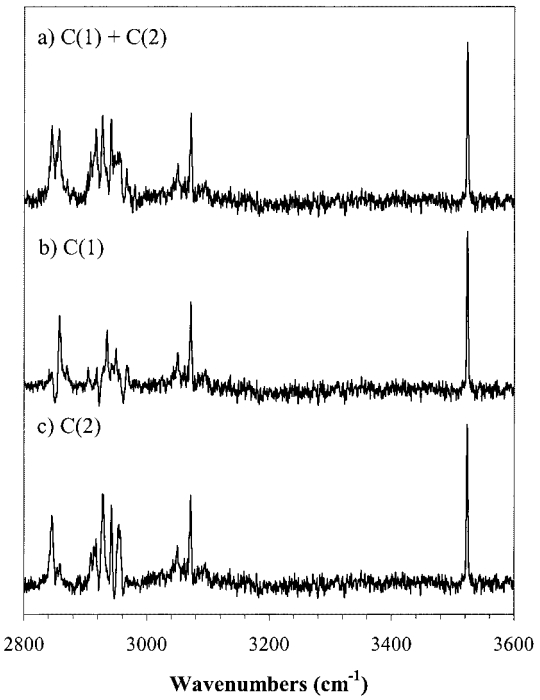

Figure 6. Resonant ion-dip infrared spectra of conformers C (a), C(1) (b), and C(2) (c). (a) UV fixed to C origin (34 883 cm^{-1}) so the IR spectrum is a sum of two conformers. (b) UV fixed to the +413 cm^{-1} vibronic band built off the C origin (see Table 3; marked with asterisk on Figure 5). (c) UV fixed to the +422 cm^{-1} vibronic band built off the C origin (see Table 3; marked with an asterisk on Figure 5). The spectra in (b) and (c) add together to produce (a).

stretch appears at 3337 cm^{-1}. The set of transitions in the 3000−3125 cm^{-1} region of each spectrum can be assigned to the aromatic C−H stretch fundamentals of indole. As with the indole N−H stretch modes, no conformation-dependent frequency shifts can be observed for these bands, as one might have anticipated.

Finally, the bands in the 2800−3000 cm^{-1} region are due to the alkyl CH stretch modes of the ethylamine side chain. One anticipates observing four transitions in this region because of what are nominally symmetric and antisymmetric stretch modes of the α and β CH_2 groups. However, the number of resolved transitions in this region varies from one conformer to the next, indicative of Fermi resonance splittings of some of the bands via coupling with overtones and combination bands of the CH bends. Despite this complication, there is clear evidence from the spectra that the alkyl CH stretch region is sensitive to the conformation of the ethylamine side chain in tryptamine.

The spectrum of conformer C(1) (Figure 7c) suffers from some interference at IR wavelengths corresponding to the strong CH stretch transitions of conformer A (Figure 7a). The interference produces small *gain* signals at the frequencies of the A CH stretch bands, presumably arising from warm TRA(A) absorbing at the ultraviolet wavelength used to monitor TRA(C1).

The spectra in Figures 7 and 8 are grouped into subsets of spectra that have a similar appearance to their alkyl CH stretch regions. These similarities are most striking for the triad of conformers in Figure 8 (B, E, and F). Conformers A and C(2) also have spectra that bear a distinct resemblance to one another (Figure 7a,b). Unfortunately, the interferences present in the spectrum of C(1) hinder comparison with that of the remaining conformer, D (Figure 7c,d). Nevertheless, the natural separation of the spectra is into a set of three and two sets of two spectra.

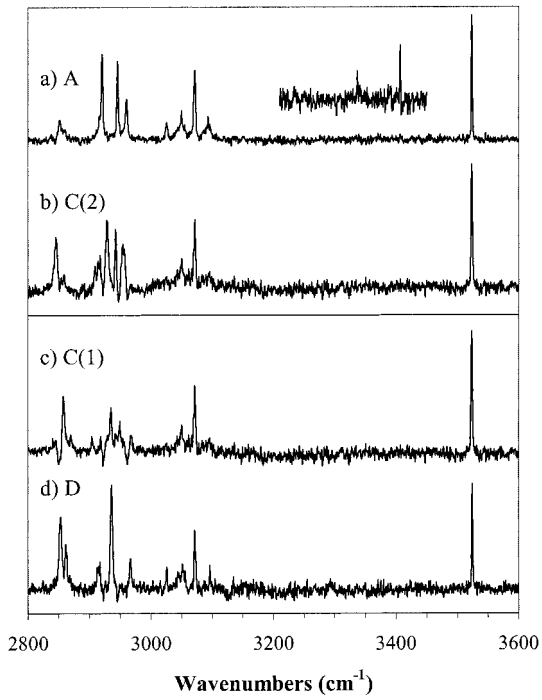

Figure 7. Resonant ion-dip infrared spectra of conformers A (a), C(2) (b), C(1) (c), and D (d). The $S_1 \leftarrow S_0$ origins of A and D were used in the RIDIR scans of A and D (see Table 3). The spectra are divided into two groups of two based on the similarities observed in the alkyl CH stretch region (A/C(2) and C(1)/D). The inset in part (a) was taken at 25 times higher sensitivity. Transitions due to the NH_2 symmetric and antisymmetric stretch fundamentals are observed at this sensitivity.

We will return to this point when we take up the final assignments in the Discussion section.

D. Calculated Vibrational Frequencies and IR Intensities. The vibrational frequencies and infrared intensities of a select subset of the vibrations of tryptamine are collected in Table 4. In the table, the computed vibrational frequencies have been scaled by 0.9603 to compare with experiment. This scale factor was chosen to best match the experimental frequencies in the indole CH and NH stretch regions. Only the low-frequency vibrations below 700 cm^{-1} and the high-frequency hydride stretch vibrations are included in the table. The low-frequency vibrations are most relevant to the ultraviolet spectroscopy, whereas the hydride stretch vibrations are probed in the RIDIR experiment. Stick diagrams of the scaled vibrational frequencies and IR intensities in the hydride stretch region of the seven lowest-energy conformers are shown in Figure 9 for comparison with experiment.

In keeping with the experimental spectra, the calculated hydride stretch transitions can be grouped into regions associated with the indole N−H ($3524^{-1} \pm 1$ cm^{-1}), the amino symmetric and antisymmetric N−H stretches (3335 ± 5 and 3418 ± 5 cm^{-1}, respectively), the aromatic C−H stretches (3040−3160 cm^{-1}), and the alkyl C−H stretches (2840−2975 cm^{-1}). The indole N−H stretch is calculated to be constant (within 1 cm^{-1}) in all conformers, just is observed experimentally. The amino NH_2 stretch vibrations are calculated to be very weak in intensity, almost a factor of 50 less than the alkyl C−H stretch vibrations. This weakness makes these vibrations difficult to observe in the RIDIR experiment, as we noted in the discussion (section C) of conformer A's RIDIR spectrum.

The ethylamine alkyl C−H stretches, which form the primary focus of the present work, show characteristic frequency and intensity patterns that reflect the configuration of the ethylamine side chain. According to the calculations, the major determiner of the alkyl CH stretch region of the IR spectrum is the *orientation* of the amino group relative to the alkyl chain and the π cloud. The amino group *position* (anti or gauche) plays a secondary role. The spectra can be divided into three groups based on the similarities of the alkyl CH stretch transitions:

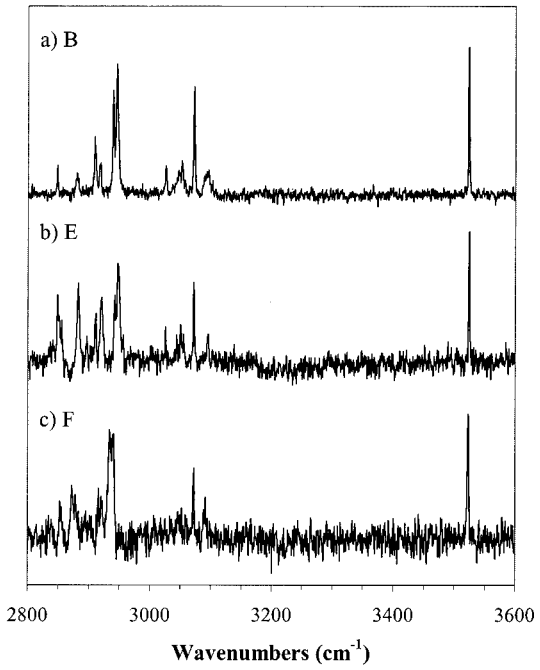

Figure 8. Resonant ion-dip infrared spectra of conformers B (a), E (b), and F (c). In each case, the $S_1 \leftarrow S_0$ origins were used as constant ion sources for RIDIR scans. This group of three spectra exhibits similar transitions in the alkyl CH stretch region.

(1) the three "lone-pair up" conformers (Gpy(up), anti(up), and Gph(up)) in Figure 9a−c; (2) the two gauche "lone-pair out" conformers (GPy(out), GPh(out)) in Figure 9d,e; and (3) the two remaining anti structures in Figure 9f,g (anti(ph), anti(py)).

The two gauche "lone-pair out" conformers (category (ii)) have calculated spectra that are nearly identical to one another, as do two of the anti structures (category (3)). In both cases, the similarity in the CH stretch spectra appears as a natural consequence of the similar amino group orientation within each pair. The three conformers in category (1) share a common amino group orientation (up), but differ in amino group position. Here, two of the three spectra (Figure 9a,b) are also almost indistinguishable from one another, whereas the third (Figure 9c), GPh(up)), is similar in the frequencies of the transitions, but differs in their intensities. In all three of the "lone-pair up" spectra, the $CH_2(\alpha)$ symmetric stretch is shifted to higher frequency than it is for the "out", "ph", and "py" conformers. As a result, all four CH stretch bands appear above 2890 cm^{-1} for the "up" isomers. Notably, the suggested grouping of the calculated spectra is similar to that in the experimental RIDIR spectra, forming the basis for the assignments proposed in the following section.

IV. Discussion

A. Assignment of the Bands to Individual Conformers. The assignment of the transitions in Figure 4 to individual conformers of tryptamine hinges on evidence from several sources, including ultraviolet spectroscopy, RIDIR spectroscopy, calculations, and past work on tryptamine and related molecules. When we initiated this study of conformation-specific infrared

TABLE 4: Summary of the Calculated Harmonic Infrared Frequencies and Intensities for the Seven Lowest-Energy Tryptamine Conformers, Using the Becke3LYP/6-31+G*(5d) Level of Theory[a]

	Gpy(out)		Gpy(up)		Anti(py)		Anti(up)		Anti(ph)		Gph(out)		Gph(up)	
	freq	int	freq	int	freq	int	freq	int	freq	int	freq	int	freq	int
low freq vib[b]	40	1.6	38	0.4	57	1.5	56	0.7	57	0.4	49	0.6	45	0.7
	80	0.9	77	0.6	80	3.7	79	1.3	73	3.3	84	0.5	77	0.2
	130	3.8	125	1.9	89	3.3	89	2.4	84	4.8	122	4.2	122	2.2
	172	5.7	170	4.9	191	2.9	190	5.2	191	4.3	196	2.4	189	5.9
	215	16.3	216	9.6	217	11.3	216	8.3	217	4.0	211	11.6	213	9.0
	241	39.8	240	14.1	230	3.4	228	2.0	221	11.0	223	2.4	229	6.9
	263	26.8	281	21.5	241	39.2	278	49.0	224	30.7	282	69.7	298	16.6
	322	49.7	315	26.8	318	15.6	313	21.9	316	27.5	321	58.9	320	35.2
	372	36.3	366	80.3	333	35.6	327	21.8	334	23.4	371	36.8	370	80.3
	418	4.8	420	3.8	397	47.9	396	47.6	397	44.5	420	2.3	418	3.5
	444	16.0	442	3.5	420	5.4	419	5.4	420	5.5	445	17.5	441	2.5
alkyl C−H[c]	***2856***	89.6	2894	42.4	***2862***	66.3	2892	46.1	***2852***	77.1	***2841***	76.8	2899	35.1
	2912	31.4	***2924***	23.4	2892	35.1	2926	19.1	2906	44.4	2912	22.5	***2916***	45.5
	2947	53.5	2934	55.9	2949	20.9	***2933***	36.0	2943	16.2	2942	77.5	2934	54.2
	2961	30.8	2968	53.2	2964	38.8	2975	36.5	2965	35.4	2954	27.7	2958	51.3
indole C−H	3050	4.1	3053	3.0	3052	3.6	3051	3.8	3052	3.6	3052	2.8	3052	4.0
	3058	4.0	3059	4.6	3057	4.5	3057	4.1	3059	6.0	3062	17.9	3057	4.2
	3069	35.2	3070	35.3	3068	39.0	3068	37.9	3069	35.9	3075	28.9	3068	36.8
	3080	37.5	3081	23.6	3080	24.5	3079	24.0	3080	21.8	3084	15.1	3079	23.2
	3136	1.0	3131	2.2	3131	2.0	3129	2.5	3129	2.5	3129	2.2	3129	2.0
NH2 (SS)	3341	0 4	3333	0.7	3337	1.0	3336	1.6	3338	0.8	3343	1.0	3340	0.6
NH2 (AS)	3424	0.8	3416	0.6	3420	0.4	3418	0.1	3420	0.5	3423	1.6	3422	1.3
N−H	3524	59.1	3524	63.8	3525	64.0	3524	64.4	3525	61.7	3523	62.8	3523	64.9

[a] Calculated frequencies are scaled by 0.9603. [b] Calculated ground-state (S_0) low-frequency vibrational modes are used to compare to S_1 state vibronic bands observed in hole-burning spectra. [c] The symmetric stretch of the α CH_2 group on the ethylamine side chain is highlighted for each structure, showing the conformational sensitivity of this mode.

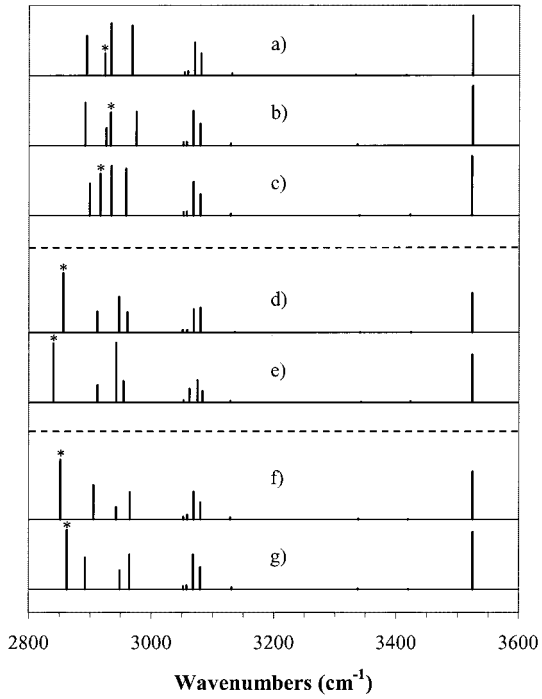

Figure 9. Calculated harmonic vibrational frequencies (scaling factor = 0.9603) and intensities for the CH and NH stretch modes of the seven lowest energy TRA structural minima. The data are presented in the following manner: (a) Gpy(up), (b) anti(up), (c) Gph(up); (e) Gpy(out), (f) Gph(out); (g) anti(ph), (h) anti (py). The symmetric stretch of the C_α hydrogens is marked with an asterisk in each case.

spectroscopy, tryptamine served as a useful starting point partly because the conformational assignments seemed largely to be in hand, allowing clear deductions about the infrared spectroscopy from known structures. However, in the process of this study, we have found it necessary to make a partial reassignment of the conformations responsible for the seven observed transitions. In this section, the evidence for the proposed assignments is outlined.

1. R2PI Spectroscopy in the S_1←S_0 Origin Region. The R2PI and UV−UV hole-burning spectroscopy in this work confirms the deduction made in earlier studies[27] that there are seven distinct origins due to seven conformational isomers of tryptamine. The Becke3LYP DFT calculations, both at the 6-31+G*(5d) and aug-cc-pVDZ basis sets, make a clear prediction that seven of the nine possible conformers of tryptamine are substantially lower in energy than the other two, consistent with observation. No minima were found at either level of theory corresponding to either of the eclipsed conformations deduced for bands D and E by the rotational-band contour analysis of Philips et al.[27]

The observation of seven conformers in tryptamine is consistent with the recent analysis of the R2PI spectrum of 4-methoxyphenethylamine[13] (4-MPEA), which shares the same ethylamine side chain as tryptamine, but anchors this side chain to a phenyl ring rather than indole. The methoxy group in 4-MPEA plays the same role as the indole ring in providing a means of distinction between the two gauche structures for the ethylamine side chain. Like tryptamine, 4-MPEA shows seven distinct origins. These seven origins have been assigned to three anti structures and two sets of two gauche structures.

2. Structural Deductions from Previous Work. Previous structural evidence for the conformers responsible for the seven observed S_1←S_0 origins in tryptamine comes from a combination of high-resolution ultraviolet spectroscopy from the Levy group[23,27] and the rotational coherence measurements of Felker and co-workers.[22] Felker and co-workers give an accurate value (±1%) of B'_{ave}, the average rotational constant in the excited state ($B'_{ave} = 1/2(B' + C')$. These are collected in Table 5. From the rotational-band contour analysis of Levy and co-workers, B'_{ave} is known to vary only slightly from B''_{ave}, which we calculate from the B'' and C'' rotational constants in Table 1 (aug-cc-pVDZ values) and report in Table 5. These B''_{ave} values are also accurately determined results of the rotational fitting of the S_1←S_0 origin bands,[27] which are predominantly A-type

TABLE 5: Comparison of the Calculated and the Experimentally Determined Rotational Constants (in GHz) for the Seven Conformers of Tryptamine: $B''_{ave} = 1/2(B'' + C'')$

description	assignment[b]	B''_{ave} (calc[c])	B'_{ave} (exp[d])	B''_{ave} (exp[e])
Gpy(out)	A	0.601	0.612	0.613
Gpy(up)	B	0.600		0.607
Anti(py)	C(1)	0.535	0.541	
Anti(up)	E	0.534	0.541	0.541
Anti(ph)	D	0.536	0.543	0.543
Gph(out)	C(2)	0.646	0.650	
Gph(up)	F	0.632		0.654

[a] Refer to Table 1 or text for structural descriptions. [b] Temporary assignments are made, based on the discussed UV spectroscopy and calculated energetics, into groups with similar amino *positions*. See discussion of RIDIR spectra for *orientation* assignments. C(1) corresponds to C′ and C(2) corresponds to C in ref 22. [c] Values calculated in this work at the Becke3LYP/aug-cc-pVDZ level of theory. [d] Experimentally determined values of the excited-state B'_{ave} rotational constants are from the Felker group (ref 22). [e] Experimentally determined values of the ground-state B''_{ave} rotational constants are from the Levy group (ref 27).

bands of a near-prolate symmetric top.[50] The experimentally determined B''_{ave} values from Philips et al.[27] are also included in Table 5. Where the two methods have been applied to the same conformer, the correspondence is excellent. Furthermore, the comparison of the experimental values of B''_{ave} with those calculated in this work shows that the calculations reproduce the experimental values to within about 2%.

This comparison thereby provides a clear basis for assignment of the *positions* of the amino groups in conformers A−F. As deduced by Levy and co-workers from their full rotational analysis, conformers A and B are both Gpy structures with $B''_{ave} = 0.61$ GHz. Conformer F and one of the bands contributing to band C are Gph isomers with $B'' = 0.65$ GHz, also consistent with the previous assignments from band contour[27] and rotational coherence measurements.[22] Furthermore, bands D, E, and C(1) can be assigned as anti structures (with $B''_{ave} = 0.54$ GHz). Bands D and E were assigned previously to structures in which the amino group is eclipsed with the C_α hydrogens. However, the postulation of such an unusual structure seems to be unnecessary in light of the excellent correspondence between experiment and theory on B''_{ave}. These eclipsed geometries have not been replicated by molecular mechanics[18] or previous ab initio calculations.[51] As a result, in what follows, we assume that the conformers responsible for transitions D and E are anti structures. In so doing, we retrieve the expected set of three anti structures (C(1), D, and E) to complement the two sets of two gauche structures (A/B as Gpy and C(2)/F as Gph).

The values of B''_{ave} cannot be used reliably to distinguish among conformers differing only in the *orientation* of the amino group (i.e., Gpy(in) from Gpy(out)), because only light H-atom motion is involved in such reorientation. However, on the basis of deuteration studies of the amino group, Wu et al.[23] tentatively assigned conformers A and B to the Gpy(up) and Gpy(out) structures, respectively. On the basis of a similar analysis, conformer F was assigned as Gph(out). Alternative orientational assignments based on the present work are included in Table 5. The basis for these assignments will be taken up shortly.

The reassignment of D, E, and C(1) to anti conformers is consistent with the positions of these three bands in the ultraviolet. As others have suggested previously,[27] the remote position of the amino group would suggest that these isomers have $S_1 \leftarrow S_0$ origins close to that in 3-methylindole (3-MI), indicated by an arrow in Figure 4. Furthermore, one might anticipate that the anti(ph) and anti(py) pair would produce $S_1 \leftarrow S_0$ origins that are nearly degenerate with one another, while the anti(up) structure would be slightly different. On this basis, an initial assignment of the three anti structures would be to associate C(1) and D with the anti(ph/py) pair, and E with the anti(up) structure.

3. Input to the Conformational Assignment from the RIDIR Spectra. A major goal of the present study is to correlate and understand the unique patterns of the alkyl CH stretch RIDIR spectra of individual conformers in terms of specific structural features of the ethylamine side chain. One hopes that such patterns will carry over to other molecules possessing conformational flexibility, and perhaps even survive the transition from the cold gas phase to room-temperature solution.

A natural grouping of the conformers into a set of three and two sets of two structures has become apparent. However, the makeup of these groups depends on whether they are categorized by amino group *position* (three anti, two Gpy, and two Gph) or amino group *orientation* (three lone-pair up, two lone pair out, and two side-ways-pointing anti structures). The reader is referred to Figure 3 for the pictures of the structures.

Unfortunately, the calculated CH stretch vibrational frequencies and infrared intensities do not reproduce the experimental spectra quantitatively, because the harmonic frequency calculations do not account for Fermi resonance mixing between the CH stretch modes and the CH bend overtones, which split and shift the experimental transitions. Furthermore, the close spacing of the computed CH stretch modes requires a high degree of accuracy in the computed CH stretch force field to retrieve the correct form of the CH stretch normal modes, whose C(α)/C(β) mixing and composition are highly sensitive to even subtle changes in the ethylamine configuration. In light of these limitations, the results of the calculations will be used instead primarily as a guide to the overall changes anticipated in the alkyl CH stretch spectrum with changing conformation, and as a means to assess which conformations are expected to have similar CH stretch spectra.

The calculations predict that the infrared spectra will be most sensitive to the amino group *orientation* rather than its *position*, which the experimental RIDIR spectra confirm. For instance, conformers A and B share the same Gpy amino group position, but have very different CH stretch RIDIR spectra (Figure 7a versus 8a). Similarly, conformers D and E are both anti structures, but their infrared spectra are also quite different (Figures 7d and 8b). Instead, the triad of spectra due to conformers B, E, and F are assigned to three different amino group positions (Gpy, anti, and Gph, respectively), yet they have similar alkyl CH stretch spectra. Based on the calculations, this similarity reflects the similar orientation of the amino group. We therefore assign the transitions B, E, and F to the three 'lone-pair up' conformers Gpy(up), anti(up), and Gph(up), respectively. Using similar reasoning, the resemblance in the RIDIR spectra between the Gpy conformer A and the Gph conformer C(2) lead us to assign them to conformers possessing similar amino group orientations, namely Gpy(out) and Gph(out). This leaves the anti (ph/py) pair as responsible for transitions C(1) and D, consistent with their initial assignment based on the positions of the UV origin transitions. A summary of the RIDIR peaks in the alkyl CH stretch region is collected in Table 6.

Thus, the RIDIR spectra, together with DFT calculations, leads to a partial reassignment of the TRA conformational isomers responsible for transitions A−F in the ultraviolet spectrum.[23] The most notable change involves the assignment of conformers D and E to anti structures. The other changes involve reassignments of the orientations of the amino groups,

TABLE 6: Experimental Transition Frequencies and Infrared Intensities in the Alkyl CH Stretch Region

origin[a]	frequency[b]	int[c]	origin[a]	frequency[b]	int[c]
A	2852	w	B	2848	w
	2920	s		2880	w
	2945	s		2909	m
	2960	m		2919	w
				2939	s
C(2)	2845	m		2945	s
	2929	s	E	2848	m
	2942	s		2855	m
	2954	m		2882	s
				2911	m
C(1)	2858	s		2921	s
	2935	m		2942	s
	2949	m		2947	s
	2968	w	F	2853	w
				2872	m
D	2853	s		2878	m
	2861	m		2916	m
	2916	w		2920	m
	2935	s		2933	s
	2966	w		2940	s

[a] See Table 3 for origin positions [b] Wavenumber values from RIDIR spectra in the alkyl C−H stretch region [c] s = strong, m = moderate, w = weak.

switching the orientations of the Gpy conformers A and B, and changing conformer F from Gph(out) to Gph(up).

B. Conformation-Specific IR and UV Spectroscopy. In the previous section, it was deduced that the alkyl CH stretch IR spectrum is particularly sensitive to the amino group *orientation* rather than its *position*. On the other hand, experiments based on analysis of rotational structure will be most sensitive to the *positions* of the amino groups of the seven conformers, but will be relatively insensitive to the much more subtle change in rotational constants associated with conformers differing only in the amino group *orientation*. The initial assignments based on the rotational spectroscopy (section A) have already been used in precisely this way to identify the amino group *positions* of the seven conformers. The CH stretch IR spectrum thus serves as a probe of conformation that is complementary to rotational spectroscopy.

The fact that the infrared frequencies and intensities are most sensitive to the amino group orientation suggests that it is the interaction of the α CH_2 group with the lone pair on nitrogen that produces the greatest effect on the vibrational frequencies. Indeed, according to the calculations (Table 4), it is the CH_2-(α) symmetric stretch (SS(α)) vibration that is particularly sensitive to the amino group orientation, shifting to higher frequencies by as much as 70 cm^{-1} when the lone pair bisects the C(α) hydrogens. The CH_2(α) symmetric stretch is marked with an asterisk in each stick spectrum of Figure 9. Unfortunately, the presence of Fermi resonance mixing and the close proximity of the α and β carbon CH stretch vibrations make it difficult to sort out whether this same effect is responsible for the changes observed in the RIDIR spectra. Deuterium substitution on the β carbon would be especially helpful in this regard. Such experiments also would facilitate a better understanding of which anharmonic couplings dominate the Fermi resonance mixing that is observed.

Because it is the lone pair on nitrogen that plays a crucial role in the CH stretch spectrum, one might anticipate a sensitivity of the CH stretch region to H-bonding at this site. We will report elsewhere on the RIDIR spectra of tryptamine-W_n clusters in which the water molecule(s) bind at the NH_2 group of tryptamine. These spectra demonstrate the sensitivity of the CH stretch spectrum to such H-bonding interactions and provide an example in which water directs the structural landscape of this amino acid model.

As far as the ultraviolet spectrum is concerned, the present work has provided UV−UV hole-burning spectra of the individual conformers, thereby dissecting an otherwise complicated and entangled set of seven UV spectra into their component parts. The positions of the $S_1 \leftarrow S_0$ origins in Figure 4 reflect these conformations. As noted already, the three anti isomers (C(1), D, and E) appear close to the origin of 3-methylindole, consistent with the remote orientation of the amino group relative to the indole π cloud. The similar intensities of the D and E bands reflect their similar energies and suggest that the intensity ascribable to conformer C(1) in band C is similar as well. The two Gpy conformers A and B dominate the spectrum, consistent with their calculated stabilities relative to the other conformers. Their $S_1 \leftarrow S_0$ origins are shifted to the blue from the 3-MI origin by +42 and +22 cm^{-1}, respectively, suggesting that the weak π H-bonding of the amino hydrogen with the π cloud on the pyrrole ring has this effect. On the other hand, the analogous π H-bonding on the phenyl side has the opposite effect, redshifting the origin of F by −42 cm^{-1}. At the same time, the Gph(out) conformer, C(2), does not have this same effect, as one might expect if it is the direction of the amino group's dipole relative to the cloud which dictates the magnitude of the electronic frequency shift.

These spectral shifts provide a foundation for understanding the effects that various conformations of the side chains have on the indole chromophore and its electronic states. In particular, one sees that the relative energies of the conformations are substantially different in the $S_1(^1L_b)$ state than they are in the ground state. Conformation F, with its small intensity, is a high-energy conformation in the ground state, but is selectively stabilized in S_1. At the same time, conformers A and B, with their large stability in S_0, are shifted to the blue, and thus are destabilized in S_1.

The $S_2(^1L_a)$ state, with its large dipole moment,[52] would be expected to exhibit an even greater sensitivity to conformation. While the present results do not identify the ^1L_a origins in these conformers, the hole-burning spectra identify which transitions are due to which conformers, providing a basis for future studies addressing the location of the ^1L_a state in each conformer.

Finally, the vibronic spectra of the individual conformers reflect the unique Franck−Condon (FC) activity that accompanies the various orientations of the ethylamine side chain relative to indole. Because the $S_1 \leftarrow S_0$ spectrum of tryptamine is a $\pi^* \leftarrow \pi$ transition localized on the indole ring, much of the Franck−Condon activity would be expected to involve the ethylamine side chain only peripherally. Nevertheless, the gauche conformers do interact with indole's π cloud to some extent, suggesting that some of these vibrations could gain FC activity and be conformation-specific. We will use the calculated ground-state vibrational frequencies and motions as a rough guide for the large amplitude motions observed in S_1.

The hole-burning spectra of Figure 5 most clearly show the conformer-specific UV spectra of tryptamine. Several examples illustrate the point. First, the two Gpy conformers A and B uniquely show activity in a 40 cm^{-1} vibration. This low-frequency vibration is predicted by the ground-state calculation (Table 4) to be a rock of the entire ethylamine side chain relative to the indole ring. It is reasonable to believe that intensity in this band could be turned on as tryptamine undergoes an excitation to S_1 because, in both A and B, the amine hydrogens are involved in a weak hydrogen bond with the indole π cloud.

Second, the hole-burning spectrum of the blended transition C possesses intensity in a vibronic transition only 120 cm^{-1} above the origin. In the ground state, calculations predict a vibration in this low frequency region for all gauche conformers. This mode is a hindered rotation about the $C_\alpha-C_\beta$ bond, coupled with a twisting motion of the indole chromophore. Again, one might anticipate some FC activity in a mode of this type, which involves motion of the ultraviolet chromophore and the weakly bound amine group. Because band C contains contributions from the Gph(out) and one of the anti(ph/py) pair, the calculated frequencies of these conformers can be used to distinguish the carrier of this band as Gph(out) (or C(2)). Third, conformer F has a vibronic transition with significant intensity in a region where the other conformers do not, appearing 305 cm^{-1} above the origin. Each conformer possesses vibrational modes in this region ($\sim$320 cm^{-1}) which involve an NH_2 rock. This suggests that intensity in the NH_2 rocking motion is selectively turned on in the Gph(out) structure (conformer F).

Overall, the comparison between the calculated ground-state, low-frequency vibrations and the experimentally determined, low-frequency vibronic bands of the excited state provides more evidence to strengthen our assignments. A strong, +40 cm^{-1} band appears in the UV spectrum of both Gpy conformers, whereas the Gph conformers show FC activity in +120 and +305 cm^{-1} bands. The anti conformers show comparatively little FC activity in these large amplitude motions, given the remote postion of the side chain relative to indole. The information is not enough, by itself, to distinguish the seven conformers, but it is complementary and consistent with our conclusions. Once again, we observe a situation in which the UV spectroscopy (vibronic bands) is sensitive to the *position* of the amino group.

C. Conformer Populations and Cooling in the Supersonic Expansion. One of the powerful aspects of the supersonic expansion is its ability to resolve transitions due to individual conformers, opening the way for conformation-specific spectroscopy. However, once the assignments of transitions to individual conformations are made, the relative intensities of the transitions of the various conformers provide some measure of their relative populations. By contrast, in solution it can be difficult to determine which conformations are present and in what relative population, especially if interchange between the conformations is fast.

As long as differences in the Franck−Condon profiles or R2PI efficiency of the conformers are small or are properly accounted for, the relative intensities of the R2PI transitions of the conformers can be used to determine the conformer populations downstream in the expansion. In tryptamine, the assignments just made for bands A−F (summarized in Figure 10) can be combined with the computed relative energies of these conformers to look more carefully at the observed populations of the conformers in the expansion. It is noteworthy that the computed energies calculated with DFT Becke3LYP/6-31+G* or aug-cc-pVDZ basis sets reproduce the general energy ordering deduced from the transition intensities. More specifically, fits of the population distribution of the conformers to a Boltzmann distribution are reasonably good, and yield a best-fit temperature of about 120 K. This is significantly below the preexpansion nozzle temperature ($\sim$400 K), a discrepancy that may indicate either inaccuracy in the relative energies of the conformers or a real interconformational cooling in the expansion. If the latter is the case, it is occurring despite computed barriers to internal rotation of the amino group orientation or position that range from 500 to 1500 cm^{-1}. Further studies of such conformational cooling are clearly needed before generalizations can be drawn.

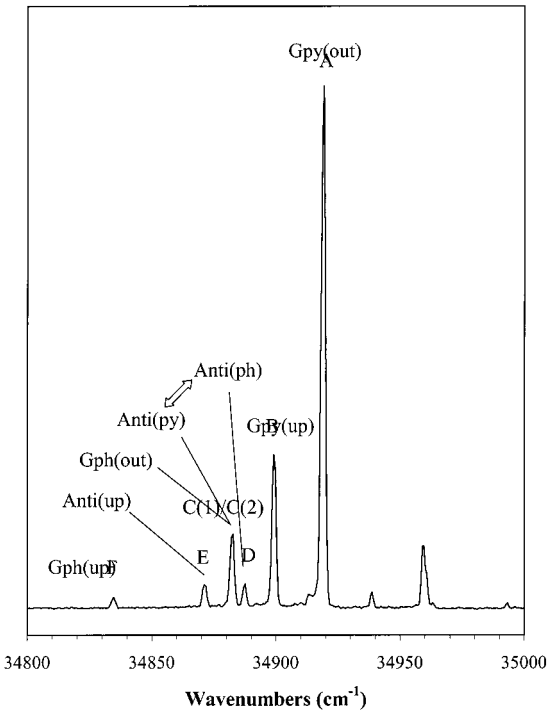

Figure 10. Final structural assignments of the seven conformers of TRA are presented with the one-color R2PI spectrum in the TRA^+ mass channel. The arrow between the anti(ph) and anti(py) pair signifies the remaining ambiguity in the conformer assignments, as we were unable to distinguish these nearly identical structures.

V. Conclusions

Conformation-specific infrared and ultraviolet spectroscopies have provided complementary information leading to a complete structural assignment of the seven ground-state conformers of tryptamine observed in a supersonic expansion. Infrared (RIDIR) spectra are sensitive to the *orientation* of the amine group on the ethylamine side chain (viewed through the CH stretch modes of the alkyl groups on the side chain), whereas rotationally resolved ultraviolet spectra are more sensitive probes of the changes in the amino group *position* relative to the indole chromophore. It appears that the CH stretch region of the IR spectrum can be used to probe the conformations of alkyl side chains containing various functional groups. More generally, the infrared spectrum should also be quite sensitive to intramolecular H-bonds when such can exist.

Density functional theory calculations aid in the assignment of these conformers, providing a prediction of their energetics and a set of harmonic vibrational frequencies to compare against RIDIR spectra. However, the CH stretch region of the infrared is particularly susceptible to Fermi resonant mixings, which confound the direct comparison of experiment with theory. The present results give some confidence in the accuracy of DFT Becke3LYP calculations for predicting the relative energies of conformers. However, further studies of conformation-specific spectra are clearly needed before the reliability of these calculations is known to be generally true. It is hoped that conformation-specific spectroscopy of the type employed here can provide a valuable testing ground in the future for the molecular mechanics force fields that are so widely used in biochemical modeling.

Acknowledgment. The authors gratefully acknowledge support for this work from the National Science Foundation (NSF-9728636-CHE).

References and Notes

(1) MacKerell, A. D.; Banavali, N. K. *J. Comput. Chem.* **2000**, *21*, 105.

(2) Foloppe, N.; MacKerell, A. D. *J. Comput. Chem.* **2000**, *21*, 86.

(3) Eyrich, V. A.; Standley, D. M.; Felts, A. K.; Friesner, R. A. *Proteins: Struct., Funct., Genet.* **1999**, *35*, 41.

(4) Eyrich, V. A.; Standley, D. M.; Friesner, R. A. *J. Mol. Biol.* **1999**, *288*, 725.

(5) Fredrichs, M.; Zhou, R.; Edinger, S. R.; Friesner, R. A. *J. Phys. Chem. B* **1999**, *103*, 3057.

(6) Friesner, R. A.; Murphy, R. B.; Beachy, M. D.; Ringnalda, M. N.; Pollard, W. T.; Dunietz, B. D.; Cao, Y. X. *J. Phys. Chem. A* **1999**, *103*, 1913.

(7) Rapp, C. S.; Friesner, R. A. *Proteins: Struct., Funct., Genet.* **1999**, *35*, 173.

(8) Stern, H. A.; Kaminski, G. A.; Banks, J. L.; Zhou, R.; Berne, B. J.; Friesner, R. A. *J. Phys. Chem. B* **1999**, *103*, 4730.

(9) Friesner, R. A.; Beachy, M. D. *Curr. Opin. Struct. Biol.* **1998**, *8*, 257.

(10) Standley, D. M.; Gunn, J. R.; Friesner, R. A.; McDermott, A. E. *Proteins: Struct., Funct., Genet.* **1998**, *33*, 240.

(11) Kim, K.; Friesner, R. A. *J. Am. Chem. Soc.* **1997**, *119*, 12952.

(12) Lindinger, A.; Toennies, J. P.; Vilesov, A. F. *J. Chem. Phys.* **1999**, *110*, 1429.

(13) Unamuno, I.; Fernandez, J. A.; Longarte, A.; Castano, F. Private communication.

(14) Dickinson, J. A.; Hockridge, M. R.; Kroemer, R. T.; Robertson, E. G.; Simons, J. P.; McCombie, J.; Walker, M. *J. Am. Chem. Soc.* **1998**, *120*, 2622.

(15) Dickinson, J. A.; Joireman, P. W.; Randall, R. W.; Robertson, E. G.; Simons, J. P. *J. Phys. Chem. A* **1997**, *101*, 513.

(16) McMahon, L. P.; Yu, H.; Vela, M. A.; Morales, G. A.; Shui, L.; Fronczek, F. R.; McLaughlin, M. L.; Barkley, M. D. *J. Phys. Chem. B* **1997**, *101*, 3269.

(17) Martinez, S. J., III.; Alfano, J. C.; Levy, D. H. *J. Mol. Spectrosc.* **1993**, *158*, 82.

(18) Sipior, J.; Sulkes, M. *J. Chem. Phys.* **1993**, *98*, 9389.

(19) Martinez, S., J. III; Alfano, J. C.; Levy, D. H. *J. Mol. Spectrosc.* **1992**, *156*, 421.

(20) Felker, P. M. *J. Phys. Chem.* **1992**, *96*, 7844.

(21) Martinez, S. J., III.; Alfano, J. C.; Levy, D. H. *J. Mol. Spectrosc.* **1991**, *145*, 100.

(22) Connell, L. L.; Corcoran, T. C.; Joireman, P. W.; Felker, P. M. *Chem. Phys. Lett.* **1990**, *166*, 510.

(23) Wu, Y. R.; Levy, D. H. *J. Chem. Phys.* **1989**, *91*, 5278.

(24) Tubergen, M. J.; Cable, J. R.; Levy, D. H. *J. Chem. Phys.* **1990**, *92*, 51.

(25) Cable, J. R.; Tubergen, M. J.; Levy, D. H. *J. Am. Chem. Soc.* **1989**, *111*, 9032.

(26) Philips, L. A.; Webb, S. P.; Martinez, S. J., III.; Fleming, G. R.; Levy, D. H. *J. Am. Chem. Soc.* **1988**, *110*, 1352.

(27) Philips, L. A.; Levy, D. H. *J. Chem. Phys.* **1988**, *89*, 85.

(28) Peteanu, L. A.; Levy, D. H. *J. Phys. Chem.* **1988**, *92*, 6554.

(29) Park, Y. D.; Rizzo, T. R.; Peteanu, L. A.; Levy, D. H. *J. Chem. Phys.* **1986**, *84*, 6539.

(30) Rizzo, T. R.; Park, Y. D.; Peteanu, L. A.; Levy, D. H. *J. Chem. Phys.* **1986**, *84*, 2534.

(31) Kim, W.; Schaeffer, M. W.; Lee, S.; Chung, J. S.; Felker, P. M. *J. Chem. Phys.* **1999**, *110*, 11264.

(32) Hartland, G. V.; Henson, B. F.; Venturo, V. A.; Felker, P. M. *J. Phys. Chem.* **1992**, *96*, 1164.

(33) Page, R. H.; Shen, Y. R.; Lee, Y. T. *J. Chem. Phys.* **1988**, *88*, 4621.

(34) Buchhold, K.; Reimann, B.; Djafari, S.; Barth, H. D.; Brutschy, B.; Tarakeshwar, P.; Kim, K. S. *J. Chem. Phys.* **2000**, *112*, 1844.

(35) Carney, J. R.; Zwier, T. S. *J. Phys. Chem. A* **1999**, *103*, 9943.

(36) Graham, R. J.; Kroemer, R. T.; Mons, M.; Robertson, E. G.; Snoek, L.; Simons, J. P. *J. Phys. Chem. A* **1999**, *103*, 9706.

(37) Guchhait, N.; Ebata, T.; Mikami, N. *J. Chem. Phys.* **1999**, *111*, 8438.

(38) Matsumoto, Y.; Ebata, T.; Mikami, N. *J. Chem. Phys.* **1998**, *109*, 6303.

(39) Gruenloh, C. J.; Carney, J. R.; Hagemeister, F. C.; Arrington, C. A.; Zwier, T. S.; Fredericks, S. Y.; Wood, J. T.; Jordan, K. D. *J. Chem. Phys.* **1998**, *109*, 6601.

(40) Gruenloh, C. J.; Carney, J. R.; Arrington, C. A.; Zwier, T. S.; Fredericks, S. Y.; Jordan, K. D. *Science* **1997**, *276*, 1678.

(41) Pauwels, P. J.; John, G. W. *Clin. Neuropharmacol.* **1999**, *22*, 123.

(42) Gruenloh, C. J.; Florio, G. M.; Carney, J. R.; Hagemeister, F. C.; Zwier, T. S. *J. Phys. Chem. A* **1999**, *103*, 496.

(43) Gotch, A. J.; Zwier, T. S. *J. Chem. Phys.* **1992**, *96*, 3388.

(44) Frisch, M. J.; Trucks, G. W.; Schlegel, H. B.; Scuseria, G. E.; Robb, M. A.; Cheeseman, J. R.; Zakrzewski, V. G.; Montgomery, J. A.; Stratmann, R. E.; Burant, J. C.; Dapprich, S.; Millam, J. M.; Daniels, A. D.; Kudin, K. N.; Strain, M. C.; Farkas, O.; Tomasi, J.; Barone, V.; Cossi, M.; Cammi, R.; Mennucci, B.; Pomelli, C.; Adamo, C.; Clifford, S.; Ochterski, J.; Petersson, G. A.; Ayala, P. Y.; Cui, Q.; Morokuma, K.; Malick, D. K.; Rabuck, A. D.; Raghavachari, K.; Foresman, J. B.; Cioslowski, J.; Ortiz, J. V.; Baboul, A. G.; Stefanov, B. B.; Liu, A. L.; Piskorz, P.; Komaromi, I.; Gomperts, R.; Martin, R. L.; Fox, D. J.; Keith, T.; Al-Laham, M. A.; Peng, C. Y.; Nanayakkara, A.; Gonzalez, C.; Challacombe, M.; Gill, P. M. W.; Johnson, B.; Chen, W.; Wong, M. W.; Andres, J. L.; Gonzalez, C.; Head-Gordon, M.; Replogle, E. S.; Pople, J. A. *Gaussian 98, Revision A.7*; Gaussian, Inc.: Pittsburgh, PA, 1998.

(45) Lee, C.; Yang, W.; Parr, R. G. *Phys. Rev. B* **1988**, *37*, 785.

(46) Becke, A. D. *J. Chem. Phys.* **1993**, *98*, 5648.

(47) Frisch, M. J.; Pople, J. A.; Binkley, J. S. *J. Chem. Phys.* **1984**, *80*, 3265.

(48) Woon, D. E.; Dunning, T. H. *J. Chem. Phys.* **1993**, *98*, 1358.

(49) Sun, S.; Bernstein, E. R. *J. Am. Chem. Soc.* **1996**, *118*, 5086.

(50) D. H. Levy has carried out further analysis of the rotational band contours of tryptamine in response to the present data. This analysis confirms that the contours are sensitive to $B''_{ave} = {}^1/_2(B'' + C'')$, but much less so to the absolute values of B″, C″, and A″. For example, assuming a reasonable geometry for the rest of the molecule, B″ changes from 0.0208 cm^{-1} for an anti structure to 0.0204 cm^{-1} for an eclipsed structure, while C″ changes from 0.0161 cm^{-1} (anti) to 0.0164 cm^{-1} (eclipsed). The fitting cannot determine B″ and C″ to this degree of accuracy. The structural change has a larger effect on A″ (0.0602 cm^{-1} for anti to 0.0636 cm^{-1} eclipsed). However, the magnitude of A″ has more effect on relative intensities than positions in the spectrum of this near-prolate asymmetric top. Thus, the conformational assignments presented in this paper are consistent with the high-resolution data from Philips et al. (ref 27).

(51) Smolyar, A.; Wong, C. F. *J. Mol. Struct. (THEOCHEM)* **1999**, *488*, 51.

(52) Lami, H.; Glasser, N. *J. Chem. Phys.* **1986**, *84*, 597.